

Eleni Vrochidou\*, Petros-Fotios Alvanitopoulos, Ioannis Andreadis and Anaxagoras Elenas

# Intelligent Systems for Structural Damage Assessment

https://doi.org/10.1515/jisys-2017-0193
Received May 4, 2017; previously published online February 22, 2018.

**Abstract:** This research provides a comparative study of intelligent systems in structural damage assessment after the occurrence of an earthquake. Seismic response data of a reinforced concrete structure subjected to 100 different levels of seismic excitation are utilized to study the structural damage pattern described by a well-known damage index, the maximum inter-story drift ratio (MISDR). Through a time-frequency analysis of the accelerograms, a set of seismic features is extracted. The aim of this study is to analyze the performance of three different techniques for the set of the proposed seismic features: an artificial neural network (ANN), a Mamdani-type fuzzy inference system (FIS), and a Sugeno-type FIS. The performance of the models is evaluated in terms of the mean square error (MSE) between the actual calculated and estimated MISDR values derived from the proposed models. All models provide small MSE values. Yet, the ANN model reveals a slightly better performance.

**Keywords:** Fuzzy inference system (FIS), Mamdani, Sugeno, artificial neural network (ANN), maximum interstory drift ratio (MISDR), structural damage estimation.

MSC2010: 05C90.

# 1 Introduction

This paper is motivated by the major problem of managing damages and life-saving resources in urban areas after the manifestation of an earthquake. Its goal is to estimate potential structural damage on the affected area, avoiding either non-linear dynamic analysis of structures or post-seismic inspection of buildings. Structural damages can be evaluated either in terms of classification to damage categories or in terms of numerical structural damage prediction.

In order to perform structural damage estimation, three intelligent techniques are developed. An ANN, a Mamdani-type FIS, and a Sugeno-type FIS are utilized for damage classification and numerical estimation of a widely used damage index, the MISDR. The novelty of the proposed study is the application and the comparison of the three regression models for the evaluation of damage indicator. The proposed models are able to efficiently quantify the structural damage by utilizing a set of newly introduced seismic intensity parameters. Previous studies confirmed the strong correlation of the aforementioned set of seismic parameters with MISDR.

This paper underlines the differences between the three schemes and shows the better choice for the problem under study. It is of major importance to identify the most accurate and efficient intelligent scheme for the damage assessment, as the estimation is inextricably associated to potential human loses and essential for the repair actions after a seismic event. Such actions must occur within a short time after the earthquake,

<sup>\*</sup>Corresponding author: Eleni Vrochidou, Department of Electrical and Computer Engineering, Democritus University of Thrace, GR-67100 Xanthi, Greece, Tel.: +30 6947 181 886, e-mail: evrochid@ee.duth.gr

Petros-Fotios Alvanitopoulos and Ioannis Andreadis: Department of Electrical and Computer Engineering, Democritus University of Thrace, GR-67100 Xanthi, Greece

Anaxagoras Elenas: Department of Civil Engineering, Democritus University of Thrace, GR-67100 Xanthi, Greece

especially in urban areas, and usually they involve a considerable number of structures. Thus, it is clear that knowledge of structural adequacy in concrete constructions is indispensable.

Among the data-driven methods, fuzzy methods are able to efficiently solve complex problems and reduce upcoming uncertainties. FISs are appealing for researchers and have found applications in various fields of science [6, 16, 25]. The most appealing characteristic of fuzzy models is that they are able to describe complex and non-linear problems [24]. The fuzzy rules, which contain the input information, are easily interpretable. Furthermore, they provide a simple interface for extending the model with additional information by adding new rules or alternate the existing ones. The advantages of fuzzy techniques can be summarized as follows: (i) allow comprehensible definitions of knowledge of the system through "if-then" rules, (ii) deal with inherent uncertainties like experts' approach to problems, (iii) are based on a solid mathematical basis, and (iv) combine numerical and categorical data. Fuzzy techniques are reported in the literature for damage classification [1, 20]. ANN techniques have also been successfully employed in numerous classification procedures or object recognition and other applications [5, 10]. The proposed models are not restricted to classifying the damage into damage categories, but they numerically estimate the structural damage degree. Classification results may be misleading, as it is common to assign the damage that belongs to the edges of the predefined intervals in neighboring categories. However, by utilizing the proposed method, one can numerically evaluate the structural damage, providing the objective picture of the damage status.

The paper is organized as follows. Section 2 describes the seismic intensity feature extraction process. Section 3 presents the motivation for the comparison of the Mamdani versus Sugeno types of FIS, and shows the development of the two schemes. Section 4 presents the ANN model. Experimental results are illustrated in Section 5. Final conclusions are drawn in Section 6.

# 2 Fundamentals

This paper introduces three model schemes based on artificial intelligence techniques to relate inputs to outputs. The models receive the same set of input parameters that describe both the damage potential of seismic excitations and the characteristics of the structure under study. The structural damage degree is considered as the output of the models by means of a widely used global damage index. More specifically, the models receive as input a set of four well-known and four proposed seismic intensity parameters. These parameters are associated with the dissipated energy and the frequency content of the seismic accelerogram. The output of both models is an MISDR value that efficiently describes the seismic structural damage potential. Figure 1 demonstrates the proposed methodology for the FIS models. The seismic feature extraction process, the definition of the utilized structural damage index, and the details of the examined frame structure are provided in the following subsections.

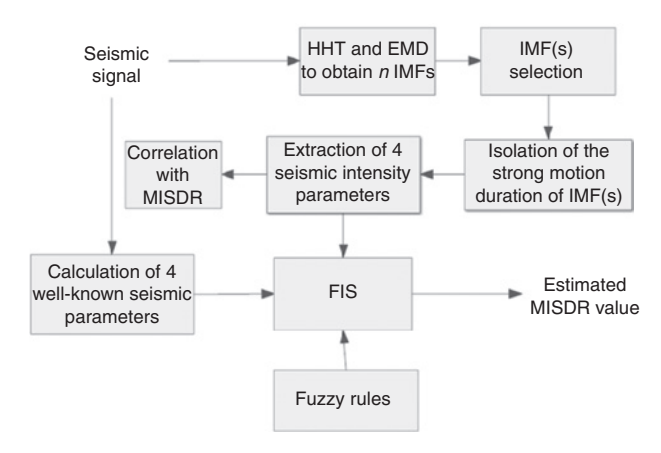


Figure 1: Proposed Methodology.

## 2.1 Seismic Intensity Feature Extraction

In this work, four well-known and four newly extracted seismic intensity parameters, calculated from the same original definitions, are utilized. Seismic intensity parameters are divided into four categories: spectral intensity, spectral, energy, and peak parameters [4]. One parameter from each category is selected and calculated for the entire seismic signal – the one that is proven to be the most correlated to MISDR [4]. These parameters are the spectrum intensity after Housner ( $SI_{u}$ ), spectral displacement (SD), Arias intensity ( $I_{s}$ ), and peak ground velocity (PGV). The same set of parameters is also calculated for a specified subsection of the initial seismic signal to form the new modified set of seismic intensity parameters, referred to as MSI, MSD, MI,, and MPGV. The proposed seismic intensity feature extraction is according to a recent methodology [22]. The process is illustrated in Figure 1 and is briefly reviewed below.

In the first step of the process, the Hilbert-Huang transform (HHT) [7] is performed. The HHT employs the ensemble empirical mode decomposition [23] to decompose the signal into a finite number of intrinsic mode functions (IMFs). For each IMF, the mean frequency value is calculated. When damage occurs to a structure, its eigenfrequency varies close to its original value. Thus, the IMF with a mean frequency value closest (within a predetermined area) to the fundamental frequency of the examined structure is selected. Supposing that f0 is the eigenfrequency of the structure, then the proposed area is between 0.9 f0 and 1.1 f0. The selected frequency band is based on the integration limits suggested by Kappos for the evaluation of spectrum intensity [8]. If the closest mean frequency value belongs to this area, then the respective IMF is selected for further analysis. If the closest mean frequency value is spaced beyond the predetermined region, then two IMFs, those that are located in either side of the region, are selected and summed.

In the second step of the process, an appropriate time-window of the selected IMF(s) is isolated. Two thresholds are specified for the time-window:  $t_{min}$  and  $t_{max}$ . The  $t_{min}$  value is set to the time when the Husid diagram reaches the value 0.05, which is equal to the time when MISDR reaches the value 0.05, which is 10% of the low-damage category threshold (set to 0.5) (Table 1). The  $t_{\rm max}$  value is the time when the Husid diagram reaches 80% of its maximum value, which is almost equal to the time when MISDR reaches 90% of its maximum value. The introduction of the time window helps reduce the computational burden, as, instead of the entire signal, only a part of one or two IMFs is imported to the following computer-supported analysis. Additionally, it represents a part of the earthquake duration where most of the seismic energy is released. Moreover, the time window is directly related to the damage evolution of the examined structure. Finally, it helps eliminate the end-effects issue [7], one reported drawback of HHT, as the IMF edges are cut off. In this strong motion time window, the four aforementioned proposed seismic intensity parameters are calculated.

In the third step of the process, the set of eight seismic parameters is input to the intelligent models, and the MISDR value is estimated for 100 seismic events. The development of the FIS involves a tuning process, so as to optimize the number of membership functions (MFs). The tuning process is analyzed in Section 3.1.

## 2.2 Structural Damage Index MISDR

Damage indices summarize the damage evoked to a structure into a single value. MISDR can evaluate the level of the post-seismic damage of a structure, and it is calculated according to the following equation:

MISDR = 
$$\frac{|u|_{\text{max}}}{h}$$
100 [%], (1)

Table 1: Structural Damage States According to MISDR.

Structural damage index	Low	Medium	Large	Total
MISDR (%)	≤0.5	0.5 < MISDR ≤ 1.5	1.5 < MISDR ≤ 2.5	>2.5

where  $|u|_{max}$  is the maximum absolute inter-story drift and h is the inter-story height [17]. The intervals of MISDR values are stated in Table 1. According to the ranges provided, the damage degree is classified as low, medium, large, or total. These categories refer to insignificant, reparable, irreparable, and severe damage or breakdown of the building, respectively.

#### 2.3 Reinforced Concrete Structure Frame Model

Figure 2 demonstrates the examined reinforced concrete (RC) frame structure. The eigenfrequency of the eight-story model is 0.85 Hz. The frame is designed according to Euro-code rules EC2 and EC8 [2, 3]. The cross-sections of the beams are T-beams with 40-cm width, 20-cm slab thickness, 60-cm total beam height, and 1.45-m effective slab width. The distance between the frames of the structure is 6 m. The frame structure has been characterized as an "importance class II and ductility class medium" according to EC8. The subsoil is of type C and the region seismicity belongs to category 2. External loads are included and are incorporated into load combinations, as suggested in EC2 and EC8. After the design of frame, a non-linear dynamic analysis takes place and its structural seismic response (MISDR) is calculated through the computer program IDARC [14].

# 2.4 Correlation Analysis

The examined intelligent models predict an MISDR value based upon the inserted input data. In order to evaluate the efficiency of the seismic intensity parameters, which will be utilized subsequently as input data to the proposed models, a correlation analysis is carried out. The relation between the seismic intensity parameters and the structural damage index MISDR is investigated. For this purpose, a correlation study based on Spearman rank correlation coefficient is carried out. For a set of n measurements of X and Y, where i = 1, 2,  $\dots$ , n, the Spearman correlation coefficient is defined as

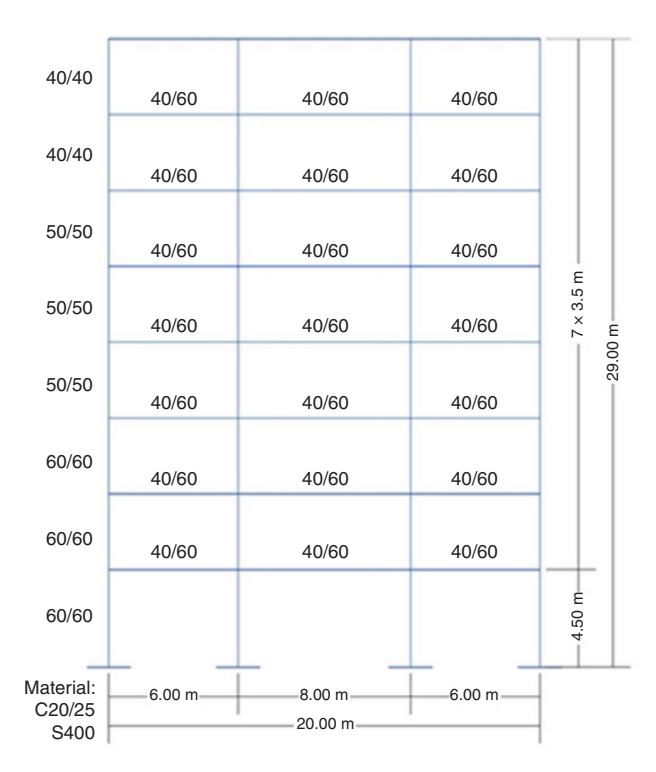


Figure 2: RC Frame Model.

Table 2: Rank Correlation Coefficients after Spearman.

Seismic parameters	I <sub>A</sub>	MI <sub>A</sub>	SI <sub>H</sub>	MSI <sub>H</sub>	SD	MSD	PGV	MPGV
MISDR	0.85	0.87	0.92	0.81	0.89	0.85	0.82	0.82

$$p_{\text{Spearman}} = 1 - \frac{6\sum_{i=1}^{n} D^2}{n(n^2 - 1)},$$
 (2)

where *D* is the difference between the ranking degree of *X* and *Y*, respectively. Correlation coefficient values >0.8 indicate a strong connection between the parameters. Values <0.45 indicate a weak connection, and all other cases between 0.45 and 0.8 reveal a medium connection [4]. The correlation degrees between MISDR and the selected seismic parameters are presented in Table 2. A strong association with MISDR is revealed for the set of seismic intensity parameters, >0.81 in all cases.

# 3 Mamdani Versus Sugeno FIS

FIS has two types based on the mathematical calculation of the inference: the Mamdani-type [11] and the Sugeno-type inference [18]. A Mamdani-type fuzzy rule is described as follows: "If A is X1 and B is X2, then C is X3," where A, B, C are variables and X1, X2, X3 are fuzzy sets. A Sugeno-type fuzzy rule is described as follows: "If A is X1 and B is X2, then C = aA + bB + c," where A, B, C are variables; and A1, A2, A3 are fuzzy sets.

The main difference between the two schemes is in the evaluation of the output MFs. In Sugeno-type FIS, the output MF is a constant or linear function (allows a single output), while in Mamdani-type it is a fuzzy set (allows multiple outputs). Mamdani-type FIS uses defuzzification technique of the fuzzy output. Sugeno-type FIS uses weighted average to compute a crisp output. Thus, Mamdani FIS provides an interpretable output. On the other hand, Sugeno FIS is more computationally efficient and has a better processing time, as the weighted average technique replaces the time-consuming defuzzification procedure. Moreover, the Sugeno FIS is more flexible, as it permits more than one parameter in the output. The output of Sugeno FIS is a function of the inputs; hence, it expresses a more distinct relation between them.

Here, the output of the model is a single numerical MISDR value. For problems of multiple inputs and of one output, both models can be equally utilized and a performance comparison between them can be provided.

# 3.1 Development of the Mamdani FIS

MISDR damage estimation is initially developed by utilizing the Mamdani-type FIS model. The model receives eight input parameters and provides one output, the MISDR estimated value. The rule base is constructed from the input-output pairs. Input and output ranges are divided into fuzzy regions. Every region is determined by an MF. The performance of the model has been tested for successive values of MFs, starting from 4. The number of MFs has been increased until the best result has been obtained. The performance of the FIS is evaluated in terms of the mean square error (MSE) between the actual calculated MISDR value and the estimated MISDR value derived from the FIS, according to the equation

$$MSE = \frac{1}{\nu} \sum_{j=1}^{\nu} |MISDR_{calculated} - MISDR_{estimated}|^2,$$
 (3)

where  $\nu$  is the number of samples (the set of examined seismic events). Figure 3 demonstrates the evolution of the average MSE for different numbers of MFs. Optimal performance is achieved for 10 MFs for input and output parameters.

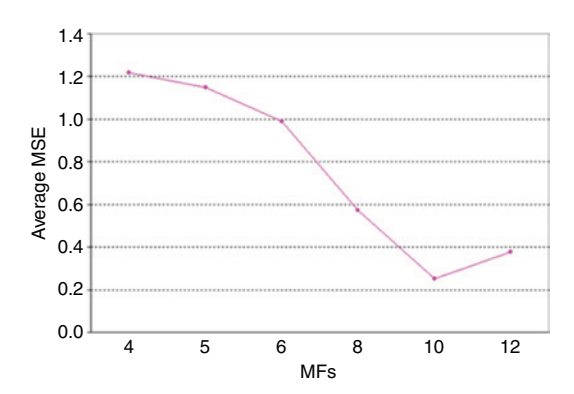


Figure 3: Average MSE for MISDR Estimation According to the Number of MFs.

The parameters that define the MFs are subsequently defined through a genetic algorithm (GA) [15]. The determination of the appropriate parameters is an optimization problem. GAs are extensively employed to resolve fuzzy optimization problems [9, 19]. Triangular MFs are utilized in this work. Defining a triangular MF is essential to designate three variables: the minimum, center, and maximum values. These values are determined from the tuning process. For eight input parameters and one output of 10 MFs each, the tuning variables rise to 270. An objective function is required to evaluate the potential solutions. The objective function in this work is the MSE between the calculated and the estimated value of MISDR defined from Eq. (3). The GA searches for the optimal solution so as to minimize the MSE. It starts with 20 individuals as initial population. The optimized parameters are encoded in a vector of double values and scaling function is set to rank. A number of genetic operators are utilized. The selection function is roulette, the crossover function is scattered, the mutation technique is Gaussian, and the migration direction is forward. The number of generations is set to 100, and fitness tolerance to the order of 10<sup>-8</sup>.

Figure 4 illustrates the evolution of the objective value during the optimization process. The GA finishes after 51 iterations due to fitness tolerance. Figure 5 demonstrates the MFs for the FIS input variables  $I_{\scriptscriptstyle A}$  and MPGV, as determined from the optimization process.

# 3.2 Development of the Sugeno FIS

The development of the MISDR damage estimation model utilizing Sugeno FIS is the same as the Mamdani FIS. In order for the two models to be directly comparable, all initial settings remain the same. The model receives the same set of information from eight input parameters and derives one output, the MISDR estima-

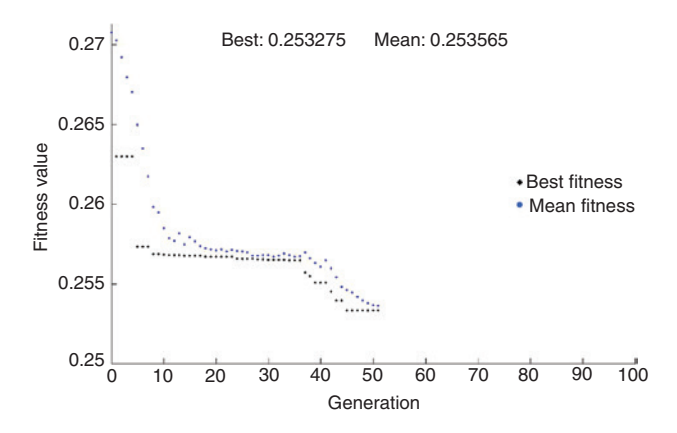


Figure 4: Evolution of Objective Value in GA Optimization.

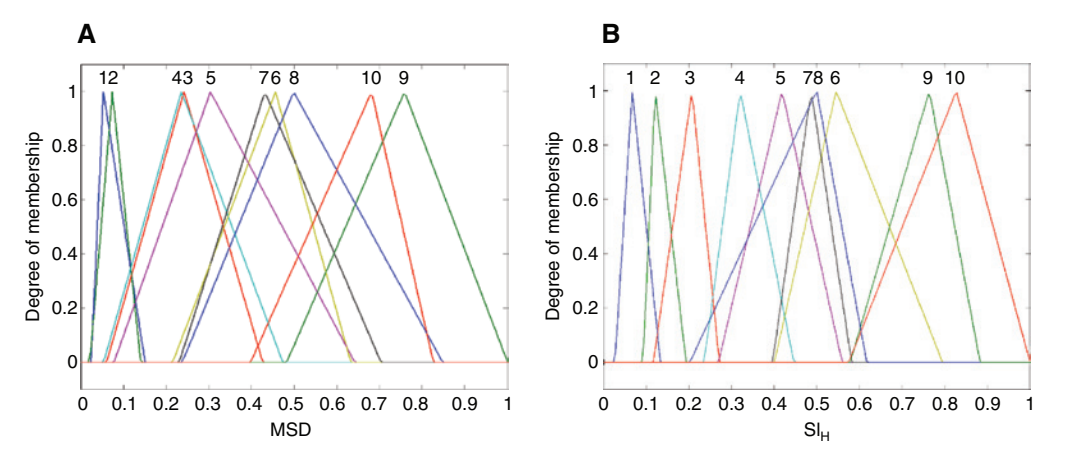


Figure 5: Ten Tuned MFs for the FIS Input Variables: (A) MSD and (B) SI...

tion value. The rule base for the Sugeno FIS is the same as for the Mamdani FIS. The triangular MFs remain the same for the input parameters, as these were defined from the optimization process.

# 4 Development of the ANN model

In an additional effort to estimate the MISDR numerically and classify seismic signals to the correct class, the aforementioned eight seismic intensity parameters are provided to construct an ANN. The ANN is a multilayer supervised feed-forward network, trained with the backpropagation learning algorithm. The goal of the net training is to minimize the MSE defined from Eq. (3). In the proposed model, each of the 100 seismic signals is represented by eight seismic intensity parameters. Thus, in the first layer of the ANN, the number of input units is set to eight. The ANN has a hidden layer of six neurons. The number of output units is set to one; a numerical value of the MISDR estimation is extracted every time. Each neuron of the hidden and output layer has a hyperbolic tangent sigmoid neural transfer function. The proposed ANN is illustrated in Figure 6.

After a neural network has been created, it must be configured. The configuration step consists of examining input and target data, setting the network's input and output sizes to match the data, and choosing settings for processing inputs and outputs that will enable best network performance. The configuration step is done automatically, when the training function is called. The selected training function for the ANN is the *trainlm*. According to the selected training function, the weight and bias values are updated according to Levenberg-Marquardt optimization [12]. It is considered as the fastest backpropagation algorithm and highly recommended among supervised algorithms. Additionally, it supports training with validation and test vectors. Validation vectors are used to stop training early if the network performance on the validation vectors fails to improve or remains the same for the maximum defined epochs in a row, set to 1000 in the present work. Test vectors are used as a further check that the network is generalizing well.

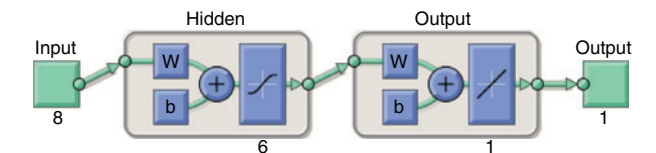


Figure 6: Proposed ANN.

Table 3: Examined Ground Motions.

No.	Earthquake [date/station/component]	MISDR calculated	No.	Earthquake [date/station/component]	MISDR calculated
1	Kobe [Jan16, 1995/KJM/000]	7.88	51	Imperial Valley [Oct15, 1979/E.C.C. FF/002]	1.48
2	Tabas (art.1) [Sep16, 1978/Tabas/LN]	6.15	52	Erzican [Mar13, 1992/Erzican/EW]	1.40
3	Tabas [Sep16, 1978/Tabas/TR]	5.95	53	Northridge [Jan17, 1994/C.Coun./000]	1.35
4	Gazli (art.1) [Mai17, 1976/Karakyr/000]	5.79	54	Erzican (art.3) [Mar13, 1992/Erzican/EW	1.29
2	Tabas [Sep16, 1978/Tabas/LN]	5.16	55	Friuli [May06, 1976/Conegliano/000	1.17
9	Gazli (art.2) [May17, 1976/Karakyr/000]	5.11	26	Coyote Lake [Aug06, 1979/C.Lk D-S.M./160]	1.04
7	Tabas (art.2) [Sep16, 1978/Tabas/LN]	4.82	57	Round Valley [Nov23, 1984/M.C.S./270]	0.95
∞	Tabas (art.1) [Sep16, 1978/Tabas/TR]	99.4	58	Kocaelli [Aug17, 1999/Duzce/180]	0.943
6	Tabas (art.3) [Sep16, 1978/Tabas/LN]	4.56	59	Baja (art.1) [Feb07, 1987/Cerro Prieto/161]	0.94
10	Kobe (arti.1) [Jan16, 1995/KJM/000]	67.4	09	Baja (art.2) [Feb07, 1987/Cerro Prieto/161]	0.91
11	Gazli (art.3) [May17, 1976/Karakyr/000]	4.28	61	Baja (art.3) [Feb07, 1987/Cerro Prieto/161]	0.89
12	Tabas (art. 1) [Sep16, 1978/Dayhook/LN]	4.21	62	Baja [Feb07, 1987/Cerro Prieto/161]	0.88
13	Kobe (art.2) [Jan16, 1995/KJM/000]	3.88	63	Oroville [Aug02, 1975/Med. Center/246]	0.87
14	Kobe (art.3) [Jan16, 1995/KJM/000]	3.84	64	Oroville (art.1) [Aug02, 1975/Med. Center/246]	0.8
15	Erzican (art.1) [Mar13, 1992/Erzican/NS]	3.65	65	Oroville (art.2) [Aug02, 1975/Med. Center/246]	0.79
16	Erzican [Mar13, 1992/Erzican/NS]	3.63	99	Oroville (art.3) [Aug02, 1975/Med. Center/246]	0.78
17	Tabas (art.2) [Sep16, 1978/Tabas/TR]	3.51	29	Victoria (art.1) [Jun09, 1980/Chihuahua/102]	0.71
18	Erzican (art.2) [Mar13, 1992/Erzican/NS]	3.34	89	Chi-Chi [Sep20, 1999/Chy025/E]	0.67
19	Tabas (art.3) [Sep16, 1978/Tabas/TR]	3.31	69	Victoria (art.2) [Jun09, 1980/Chihuahua/102]	99.0
20	Dinar [Jan10,1995/Dinar/090]	3.00	70	Victoria (art.3) [Jun09, 1980/Chihuahua/102]	0.65
21	San Salvador [Oct10, 1986/G.I.Cent./090]	2.95	71	Victoria [Jun09, 1980/Chihuahua/102]	0.64
22	Dinar (art.1) [Jan10, 1995/Dinar/090]	2.86	72	Coalinga [May02, 1983/PC.C. Sc./360]	09.0
23	Northridge (art.1) [Jan17, 1994/C.Coun./000]	2.74	73	Spitak (art.1) [Dec07, 1988/Gukasian/000]	0.57
24	Northridge (art.2) [Jan17, 1994/C.Coun./000]	2.68	74	Spitak [Dec07, 1988/Gukasian/000]	0.552
25	Victoria [Jun09, 1980/Cerro Prieto/045]	2.52	75	Spitak (art.2) [Dec07, 1988/Gukasian/000]	0.54
26	San Salvador (art.1) [Oct10, 1986/G.I.Cent./090]	2.45	9/	Tabas [Sep16, 1978/Dayhook/LN]	0.45
27	Duzce [Nov12, 1999/Bolu/000]	2.39	77	Coalinga [Jul22, 1983/CHP/000]	0.42
28	Duzce (art.1) [Nov12, 1999/Bolu/000]	2.38	78	San Fernando [Feb09, 1971/Fort Tejon/000]	0.395
29	Kobe [Jan16, 1995/Nishi-Akashi/000]	2.37	79	Hector Mine [Oct16, 1999/Amboy/000]	0.39
30	San Salvador (art.2) [Oct10, 1986/G.I.Cent./090]	2.36	80	Superstition Hills [Nov24, 1987/KRN/270]	0.38

Table 3 (continued)

No.	Earthquake [date/station/component]	MISDR calculated	No.	Earthquake [date/station/component]	MISDR calculated
31	Victoria (art.1) [Jun09, 1980/Cerro Prieto/045]	2.31	81	Mt Lewis [Mar31, 1986/Halls Valley/000]	0.37
32	Kobe (art.1) [Jan16, 1995/Nishi-Akashi/000]	2.23	82	Kocaelli [Aug17, 1999/Eregli/090]	0.35
33	Duzce (art.1) [Nov12, 1999/Duzce/180]	2.17	83	Cape Mendocino [Apr25, 1992/EM/000]	0.345
34	Duzce (art.2) [Nov12, 1999/Duzce/180]	2.13	84	Duzce [Nov12, 1999/1058/E]	0.34
35	Duzce (art.2) [Nov12, 1999/Bolu/000]	2.09	85	Loma Prieta [Oct18, 1989/C.L.D.D./195]	0.335
36	Cape Mendocino [Apr25, 1992/Cape M. /000]	2.03	98	Parkfield [Jun28, 1966/Cholame #8/050]	0.33
37	San Salvador (art.3) [Oct10, 1986/G.I.Cent./090]	2.01	87	Loma Prieta (art.1) [Oct18, 1989/UCSC/000]	0.30
38	Duzce (art.3) [Nov12, 1999/Duzce/180]	1.99	88	Loma Prieta (art.2) [Oct18, 1989/UCSC/000]	0.28
39	Duzce (art.3) [Nov12, 1999/Bolu/000]	1.98	89	Coalinga Park [May02, 1983/PF. Z16/090]	0.27
40	Victoria (art.2) [Jun09, 1980/Cerro Prieto/045]	1.93	06	Loma Prieta [Oct18, 1989/UCSC/000]	0.26
41	Dinar (art.2) [Jan10, 1995/Dinar/090]	1.85	91	Loma Prieta (art.3) [Oct18, 1989/UCSC/000]	0.25
42	Victoria (art.3) [Jun09, 1980/Cerro Prieto/045]	1.81	92	West Moreland [Apr26, 1981/B. Air./225]	0.245
43	Erzican (art.1) [Mar13, 1992/Erzican/EW]	1.79	93	Double Springs Eq [Sep12, 1994/Wood./000]	0.24
44	Erzican (art.3) [Mar13, 1992/Erzican/NS]	1.69	94	Duzce Lam [Nov12, 1999/L.st.531/N]	0.23
45	Dinar (art. 3) [Jan10, 1995/Dinar/090]	1.65	95	Hollister [Jan26, 1920/H.D. Array #1/255]	0.18
46	Erzican (art.2) [Mar13, 1992/Erzican/EW]	1.60	96	Calindar [Nov24, 1976/St. Code: 37/S49E]	0.11
47	Superstition Hills (art.1)[Nov24, 1987/KRN/270]	1.59	26	San Fransisco (art.1) [Mar22, 1957/1117/010]	0.10
48	Duzce [Nov12, 1999/Duzce/180]	1.54	86	San Fransisco [Mar22, 1957/1117/010]	0.09
65	Gazli [May17, 1976/Karakyr/000]	1.52	66	San Fransisco (art.2) [Mar22, 1957/1117/010]	0.08
20	Northridge (art.3) [Jan17, 1994/C.Coun./000]	1.51	100	Irpinia Eq [Nov23, 1980/Arienza/000]	0.07

Natural earthquakes are marked in bold font.

# **5 Experimental Results**

#### 5.1 FIS Models

A set of 100 seismic excitations, natural and artificially generated, are utilized to train and test the examined models. Natural accelerograms are derived from the Pacific Earthquake Engineering Research Center [13]. Artificial accelerograms are derived from the natural accelerograms, utilizing the methodology suggested by Vrochidou et al. [21]. The final data set of seismic excitations covers a wide range of MISDR values and displays a uniform formation: 25 accelerograms in each one of the four seismic categories according to the MISDR calculated values. Table 3 provides the necessary information (seismic event, country, date, station, and component) for the set of 100 accelerograms. In Table 3, the calculated MISDR values for the seismic events regarding the examined structure are also included.

The FIS models are trained with the eight selected seismic parameters of 99 seismic signals. One seismic signal is tested every time. Table 4 presents the MISDR estimation achieved with the Mamdani and Sugeno FIS, for every seismic event. The MSE between the estimated and the calculated value of MISDR for every

Table 4: MISDR Estimation Values with Mamdani and Sugeno FIS.

No. of	MISDR e	stimation	No. of	MISDR e	stimation	No. of	MISDR e	stimation	No. of	MISDR e	stimation
event	Mamdani	Sugeno	event	Mamdani	Sugeno	event	Mamdani	Sugeno	event	Mamdani	Sugeno
1	4.92	4.92	26	2.38	2.03	51	0.77	1.84	76	0.50	1.19
2	6.08	5.4	27	2.55	2.89	52	2.03	1.86	77	0.32	0.315
3	5.40	5.11	28	2.10	2.21	53	1.60	1.68	78	0.31	0.316
4	4.94	4.94	29	2.32	2.3	54	2.15	1.69	79	0.35	1.16
5	5.17	5.17	30	2.40	2.46	55	1.33	1.33	80	0.64	0.729
6	5.80	5.3	31	2.12	2.12	56	1.52	1.19	81	0.32	0.123
7	5.45	4.96	32	1.51	1.59	57	1.33	0.957	82	0.32	0.315
8	5.34	4.75	33	2.06	1.65	58	1.65	1.26	83	0.51	0.509
9	3.94	3.94	34	1.61	1.75	59	1.83	1.99	84	0.47	0.122
10	3.94	3.94	35	2.10	2.1	60	1.25	1.47	85	0.36	0.325
11	4.31	5.27	36	1.81	1.83	61	1.49	1.43	86	0.51	0.571
12	5.39	3.1	37	2.84	2.47	62	1.70	1.95	87	0.50	0.388
13	3.94	3.66	38	2.05	2.1	63	1.13	1.19	88	0.32	0.317
14	3.94	3.94	39	2.13	2.11	64	1.02	1.44	89	0.31	0.455
15	3.94	4.53	40	1.69	2.39	65	0.70	0.7	90	0.15	0.315
16	3.94	3.94	41	1.56	2.13	66	0.87	0.509	91	0.45	0.357
17	3.04	3.83	42	2.10	1.76	67	0.76	0.696	92	0.13	0.421
18	3.77	2.44	43	2.21	1.99	68	1.19	1.46	93	0.13	0.122
19	3.95	3.94	44	1.65	1.67	69	0.80	0.767	94	0.16	0.315
20	2.91	2.5	45	1.80	2.41	70	0.76	0.799	95	0.13	0.125
21	2.12	2.55	46	2.11	2.1	71	0.74	0.771	96	0.13	0.122
22	2.32	2.07	47	1.83	2.4	72	0.50	0.593	97	0.12	0.12
23	3.94	2.1	48	2.01	2.29	73	0.51	0.587	98	0.15	0.122
24	2.80	2.1	49	1.94	1.94	74	0.51	0.509	99	0.15	0.122
25	2.63	1.93	50	2.20	1.89	75	0.51	0.639	100	0.12	0.12
Fourth o	damage cate	gory	Third da	mage catego	ory	Second	damage cate	egory	First da	mage catego	ry
Misclas	sified	2	Misclass	sified	1	Misclas	sified	5	Misclas	sified	1
Mamda	ni:		Mamdar	ni:		Mamda	ni:		Mamda	ni:	
Misclas	sified	4	Misclass	sified	1	Misclas	sified	6	Misclas	sified	2
Sugeno	:		Sugeno	:		Sugeno	):		Sugeno	:	
Correct	classification	n rate for al	l the expe	riments with	n Mamdani-	type FIS:					91%
Correct	classification	n rate for al	I the expe	riments MSI	with Suge	no-type F	IS:				87%

Misclassified signals are marked in bold font.

Table 5: MSE with Mamdani and Sugeno FIS.

No. of		MSE	No. of		MSE	No. of		MSE	No. of		MSE
event	Mamdani	Sugeno	event	Mamdani	Sugeno	event	Mamdani	Sugeno	event	Mamdani	Sugeno
1	8.762	8.762	26	0.005	0.176	51	0.504	0.130	76	0.003	0.548
2	0.005	0.563	27	0.012	0.250	52	0.397	0.212	77	0.010	0.011
3	0.303	0.706	28	0.078	0.029	53	0.063	0.109	78	0.006	0.005
4	0.722	0.722	29	0.003	0.005	54	0.740	0.160	79	0.002	0.593
5	0.000	0.000	30	0.002	0.010	55	0.026	0.026	80	0.068	0.122
6	0.476	0.036	31	0.036	0.036	56	0.212	0.023	81	0.003	0.061
7	0.397	0.020	32	0.518	0.410	57	0.144	0.000	82	0.001	0.001
8	0.462	0.008	33	0.012	0.270	58	0.500	0.100	83	0.029	0.029
9	0.384	0.384	34	0.270	0.144	59	0.792	1.103	84	0.017	0.048
10	0.303	0.303	35	0.000	0.000	60	0.116	0.314	85	0.001	0.000
11	0.001	0.980	36	0.048	0.040	61	0.360	0.292	86	0.032	0.058
12	1.392	1.232	37	0.689	0.212	62	0.672	1.145	87	0.040	0.008
13	0.004	0.048	38	0.004	0.012	63	0.068	0.102	88	0.002	0.001
14	0.010	0.010	39	0.023	0.017	64	0.048	0.410	89	0.002	0.034
15	0.084	0.774	40	0.058	0.212	65	0.008	0.008	90	0.012	0.003
16	0.096	0.096	41	0.084	0.078	66	0.008	0.073	91	0.040	0.011
17	0.221	0.102	42	0.084	0.003	67	0.003	0.000	92	0.012	0.033
18	0.185	0.810	43	0.176	0.040	68	0.270	0.624	93	0.012	0.014
19	0.410	0.397	44	0.002	0.000	69	0.020	0.011	94	0.005	0.007
20	0.008	0.250	45	0.023	0.578	70	0.012	0.022	95	0.003	0.003
21	0.689	0.160	46	0.260	0.250	71	0.010	0.017	96	0.000	0.000
22	0.325	0.672	47	0.058	0.656	72	0.010	0.000	97	0.000	0.000
23	1.440	0.410	48	0.221	0.563	73	0.004	0.000	98	0.004	0.001
24	0.014	0.336	49	0.176	0.176	74	0.002	0.002	99	0.005	0.002
25	0.012	0.348	50	0.476	0.144	75	0.001	0.010	100	0.003	0.003
Fourth	damage cate	gory	Third dan	nage categ	ory	Second o	damage cate	egory	First dam	age catego	ry
Mean N	1SE	0.668	Mean MS	Ε	0.133	Mean MS	SE	0.198	Mean MS	Ε	0.012
Mamda	ni:		Mamdani	i:		Mamdan	i:		Mamdan	i:	
Mean N	1SE	0.725	Mean MS	Ε	0.172	Mean MS	SE	0.196	Mean MS	Ε	0.064
Sugeno	):		Sugeno:			Sugeno:			Sugeno:		
Average	e MSE for all	the experin	nents with I	Mamdani-ty	ype FIS:						0.253
Average	e MSE for all	the experin	nents MSE	with Sugen	o-type FIS:						0.289

Total average MSE for both models is marked in bold font.

seismic event with the two models is included in Table 5. The average MSE for all experiments is 0.253 with Mamdani-type FIS and 0.289 with Sugeno-type FIS. The results obtained show that for the given application of structural damage estimation, Mamdani-type FIS and Sugeno-type FIS work rather similarly.

Table 5 also presents the average MSE for every damage category separately for both models. It is obvious that for both models, the average MSE is lower in the first damage category, in the same range of values in the second and third categories, and higher in the fourth damage category. This was expected as, according to Table 1, the MISDR value range is narrow for category 1, in the same range for categories 2 and 3, and very wide for category 4. Indeed, for the fourth damage category, there is no upper limit. In order to accurately estimate the MISDR value for seismic signals that belong in this category, like in case of the seismic event no. 1 (Kobe), more seismic signals of that intensity are required. The FIS in neither model can accurately predict this value, as the training test does not comprise seismic events of that range of MISDR values.

The ability of the two models to classify the damage into damage categories is also examined according to the estimated MISDR values. In Table 4, the misclassified seismic signals are marked in bold. Correct classification rates of 91% are achieved with the Mamdani-type FIS, while 87% with the Sugeno-type FIS.

In a second experimental approach, the training process exploits 80 signals and the testing process 20 signals, randomly selected every time. The experiment takes place 100 times for statistical reasons in order

Table 6: Minimum, Median, and Maximum MSE of MISDR Estimation for 100 Trials of Randomly Selected Training and Testing Sets with Mamdani and Sugeno FIS.

	Minimum	Median	Maximum
MSE Mamdani	0.06	0.21	1.15
MSE Sugeno	0.08	0.23	1.07

to achieve convergence. Table 6 summarizes the results, presenting the minimum, maximum, and median values of the MSE utilizing both models. The minimum, maximum, and median values of the MSE are 0.06, 1.15, and 0.21, respectively, for the Mamdani-type FIS. The median value arising from the second experimental approach is close to the total average MSE value (0.253) of the first experimental approach. Similarly, the minimum, maximum, and median values of the MSE are 0.08, 1.07, and 0.23, respectively, for the Sugeno-type FIS. The median value arising from this approach is close to the total average MSE value (0.289) of the first experimental approach.

This observation justifies the use of the proposed FIS for the MISDR estimation. Based on these findings, one may claim that the Mamdani-type FIS outperforms the Sugeno-type FIS in case of the examined structural damage estimation problem.

Table 7: MISDR Estimation Values and MSE with ANN.

No. of event	MISDR estimation	MSE	No. of event	MISDR estimation	MSE	No. of event	MISDR estimation	MSE	No. of event	MISDR estimation	MSE
1	7.63	0.063	26	2.33	0.014	51	1.34	0.020	76	0.46	0.000
2	5.55	0.360	27	2.41	0.000	52	1.74	0.116	77	0.46	0.002
3	5.83	0.014	28	2.29	0.008	53	1.29	0.004	78	0.4	0.000
4	6.57	0.608	29	1.69	0.462	54	1.48	0.036	79	0.64	0.063
5	4.84	0.102	30	2.39	0.001	55	1.17	0.000	80	0.4	0.000
6	4.39	0.518	31	2.35	0.002	56	1.07	0.001	81	0.37	0.000
7	5.83	1.020	32	1.65	0.336	57	0.91	0.002	82	0.35	0.000
8	5.53	0.757	33	2.46	0.084	58	0.93	0.000	83	0.43	0.008
9	4.66	0.010	34	2.1	0.001	59	1.62	0.462	84	0.35	0.000
10	4.49	0.000	35	2.16	0.005	60	0.93	0.000	85	0.37	0.002
11	3.55	0.533	36	1.82	0.044	61	0.94	0.002	86	0.3	0.001
12	2.66	2.403	37	2.03	0.000	62	1.24	0.130	87	0.28	0.000
13	3.38	0.250	38	1.92	0.005	63	0.91	0.002	88	0.28	0.000
14	3.45	0.152	39	1.88	0.010	64	0.8	0.000	89	0.29	0.000
15	3.49	0.026	40	2.07	0.020	65	0.82	0.001	90	0.2	0.004
16	3.67	0.002	41	1.81	0.002	66	0.82	0.002	91	0.24	0.000
17	3.76	0.063	42	1.81	0.000	67	0.82	0.012	92	0.27	0.001
18	3.08	0.068	43	1.77	0.000	68	0.93	0.068	93	0.21	0.001
19	3.86	0.303	44	2.95	1.588	69	0.69	0.001	94	0.27	0.002
20	2.7	0.090	45	2.02	0.137	70	0.79	0.020	95	0.22	0.002
21	2.88	0.005	46	1.55	0.003	71	0.65	0.000	96	0.12	0.000
22	1.87	1.040	47	1.75	0.026	72	0.56	0.002	97	0.38	0.078
23	2.95	0.044	48	1.57	0.001	73	0.61	0.002	98	0.08	0.000
24	2.69	0.000	49	2.24	0.518	74	0.52	0.001	99	0.09	0.000
25	2.39	0.017	50	1.56	0.003	75	0.55	0.000	100	0.12	0.003
First da	mage category	,	Second	damage categ	ory	Third da	ımage categor	у	Fourth o	damage catego	ory
Mean M	MSE: e MSE for all th	0.338 e experim	Mean N	ISE:	0.131	Mean N	SE:	0.035	Mean M		0.007 <b>0.128</b>
_	classification	•		- *********							96%

Table 8: Comparison of the FIS and ANN Models.

	Mamdani FIS	Sugeno FIS	ANN
Average MSE	0.253	0.289	0.128
Correct classification rate	91%	87%	96%

## 5.2 ANN Model

In this work, from the set of 100 accelerograms, 83 seismic signals are utilized for training, 12 seismic signals (3 out of each one of the 4 damage categories) for validation, and 5 seismic signals for testing. The numerical results are presented in Table 7. Table 7 includes the estimated MISDR value and the MSE for every seismic signal and the average MSE for every damage category separately. The average MSE is lower in the first damage category, higher in the fourth damage category, and the same range of values in the second and third, as expected. The proposed ANN provides very low average MSE in the MISDR estimation, equal to 0.128. As it can be observed from Table 7, in most of the experiments, the MSE is significantly low. When the numerical MISDR estimation values of Table 6 are assigned to damage categories (according to Table 1), the ability of the ANN to classify the structural damage in one of the defined categories increases up to 96%. Misclassified signals are marked in Table 7 in bold font. It can be observed that misclassified signals belong, in most cases, to the edges of the predefined intervals.

### 5.3 FIS Models Versus ANN Model

The presented ANN model can be compared to the FIS model analyzed in the previous section. Both models receive the same input data and export an MISDR numerical estimation value. Table 8 is a comparative table of the results obtained with the examined models. As it can be seen from Table 8, FIS and ANN approximate the same level of performance; all models provide high classification rates and small MSE values.

It should be noted, though, that the ANN model, in the case of the examined damage assessment problem, reveals a slightly better performance. This is due to the different architecture of the models. When a small set of inputs is utilized for training the FIS, then fewer rules are obtained and the system finds difficulty in optimally mapping multiple inputs to outputs. However, as the training set increases, more rules are obtained and the FIS is able to produce more accurate estimations and, therefore, lower MSE and better classification results.

# 6 Conclusions

Classification results are not always reliable indicators of the post-earthquake status of buildings. The aim of this work is to numerically estimate the MISDR structural damage index through a time-frequency analysis of the seismic signal. A new set of seismic intensity features that quantitatively expresses the seismic energy in association with the occurred damage on a certain structure is extracted. The effectiveness of the new seismic features is numerically justified through a correlation analysis; a strong degree of interdependence between the new features and the MISDR, as a set of well-known seismic parameters, is obtained. One hundred earthquake records are utilized to test the proposed methodologies: a Mamdani-type FIS, a Sugeno-type FIS, and an ANN. One hundred natural and artificial earthquake signals are utilized to train and test the proposed models. The models are trained to estimate the MISDR value induced by a seismic signal in a certain structure. Every tested seismic signal is inserted as input to the models in terms of eight proposed seismic intensity parameters.

The Mamdani-type FIS is developed primarily. The FIS is combined with a GA to tune its MFs optimally. In the Sugeno-type FIS, MFs and rule base are designed to be the same as in the Mamdani-type FIS. Results reveal that the two models similarly perform the estimation of the MISDR value, as the average MSE of all experiments is almost the same: 0.253 for Mamdani FIS and 0.289 for Sugeno FIS. Moreover, two different approaches for training the FIS models, manually and randomly, lead to the same degree of MSE for both models. When MISDR estimation values are assigned to damage categories, correct classification of up to 91% is achieved with the Mamdani FIS, while 87% with the Sugeno FIS.

Finally, for the same set of earthquake signals, and the same input and output parameters, an ANN is developed. Experimental results reveal that the total average MSE of the MISDR estimation is equal to 0.128; results translated to classification rate correspond to 96%. FIS and ANN models approximate the same level of performance regarding the examined structural damage assessment problem.

The models proposed in this work are original and can evaluate the post-seismic damage status of buildings in the form of damage indices, avoiding complicated and time-consuming non-linear dynamic analysis. All models can be utilized by the public administration for the evaluation of damage scenarios in important buildings or regions. This is of great importance for an adequate post-seismic management of financial and other resources in the case of severe earthquakes. Another possible application of the proposed damage assessment techniques is their implementation on a microchip in combination with an accelerograph and a signal transmitting unit for the direct and real-time evaluation of damage caused by an earthquake. Until today, surveys are performed with on-site examination by expert engineers and the process is not automatic. Thus, these models could be useful tools for an online estimation of the structural damage on buildings right after the occurrence of an earthquake.

# **Bibliography**

- [1] I. Andreadis, Y. Tsiftzis and A. Elenas, Intelligent seismic acceleration signal processing for structural damage classification, IEEE Trans. Instrum. Meas. 56 (2007), 1555-1564.
- [2] EC2, Eurocode 2: design of concrete structures part 1: general rules and rules for buildings, European Committee for Standardization, Brussels, Belgium, 2000.
- [3] EC8, Eurocode 8: design of structures for earthquake resistance part 1: general rules, seismic actions, and rules for buildings, European Committee for Standardization, Brussels, Belgium, 2004.
- [4] A. Elenas, and K. Meskouris, Correlation study between seismic acceleration parameters and damage indices of structures, Eng. Struct. 23 (2001), 698-704.
- [5] L. Fausett, Fundamentals of neural networks architectures, algorithms and applications, Prentice Hall International, Upper Saddle River, NJ, 1994.
- [6] J. S. Gao, X. H. Xu and C. He, A study on the control methods based on 3-DOF helicopter model, J. Comput. 7 (2012), 2526–2533.
- [7] N. E. Huang, Z. Shen, S. R. Long, M. C. Wu, H. H. Shih, Q. Zheng, N.-C. Yen, C. C. Tung and H. H. Liu, The empirical mode decomposition and the Hilbert spectrum for nonlinear and non-stationary time series analysis, Proc. R. Soc. A 454 (1998), 903-995.
- [8] A. J. Kappos, Sensitivity of calculated inelastic seismic response to input motion characteristics, in: Proceedings of the 4th *U.S. National Conference on Earthquake Engineering*, pp. 25–34, Palm Springs, California, 1990.
- [9] M. Kaya and R. Alhajj, Genetic algorithms based optimization of membership functions for fuzzy weighted association rules mining, in: Proceedings of the 9th International Symposium on Computers and Communications, ISCC, pp. 110-115, Alexandria, Egypt, 2004.
- [10] K. M. Lam and H. Yan, Locating and extracting the eye in human face images, Pattern Recognit. 29 (1996), 771-779.
- [11] E. H. Mamdani, Applications of fuzzy logic to approximate reasoning using linguistic synthesis, IEEE Trans. Comput. 26 (1977), 1182-1191.
- [12] D. Marquardt, An algorithm for least-squares estimation of nonlinear parameters, SIAM J. Appl. Math. 11 (1963), 431–441.
- [13] PEER Ground Motion Database, Pacific Earthquake Engineering Research Center [Online], Available at: http://ngawest2. berkeley.edu/, Accessed 7 February, 2018.
- [14] A. M. Reinhorn, H. Roh, M. Sivaselvan, S. K. Kunnath, R. E. Valles, A. Madan, C. Li, R. Lobo and Y. J. Park, IDARC 2D Version 7.0: a program for inelastic damage analysis of structures, MCEER Technical Report-MCEER-09-0006, State University of New York, Buffalo, 2009.
- [15] S. N. Sivanandam and S. N. Deepa, Introduction to genetic algorithms, Springer Verlag, Germany, 2008.
- [16] Z. Y. Song, X. L. Song, C. Y. Liu and Y. B. Zhao, Research on real-time simulation and control of linear 1-stage inverted pendulum, J. Comput. 8 (2013), 896-903.
- [17] Structural Engineers Association of California (SEAOC), Vision 2000: performance based seismic engineering of buildings, Sacramento, California, 1995.

- [18] M. Sugeno, in: M. M. Gupta, G. N. Saridis and B. R. Gaines, eds., Fuzzy Measures and Fuzzy Integrals: A Survey in Fuzzy Automata and Decision Processes, North Holland, New York, 1977.
- [19] K. S. Tang, K. F. Man, Z. F. Liu and S. Kwong, Minimal fuzzy memberships and rules using hierarchical genetic algorithms, IEEE Trans. Ind. Electron. 45 (1998), 162-169.
- [20] I. Tsiftzis, I. Andreadis and A. Elenas, A Fuzzy system for seismic signal classification, IEE Proceedings-Vision, Image and Signal Processing. 153 (2006), 109-114.
- [21] E. Vrochidou, P. Alvanitopoulos, I. Andreadis, A. Elenas and K. Mallousi, Synthesis of artificial spectrum-compatible seismic accelerograms, Inst. Phys. J. Meas. Sci. Technol. 25 (2014), 1-14.
- [22] E. Vrochidou, P. Alvanitopoulos, I. Andreadis and A. Elenas, Structural damage estimation in reinforced concrete mid-rise structure based on time frequency analysis of seismic accelerograms, IET Sci. Meas. Technol. 10 (2016), 900-909.
- [23] Z. Wu and N. E. Huang, Ensemble empirical mode decomposition: a noise-assisted data analysis method, Adv. Adapt. Data Anal. 1 (2009), 1-14.
- [24] L. A. Zadeh, Fuzzy sets, Inf. Control 8 (1965), 338-353.
- [25] G. Y. Zhao, Y. Shen and Y. L. Wang, Fuzzy PID position control approach in computer numerical control machine tool, I. Comput. 8 (2013), 622-629.

# **Bionotes**

#### Eleni Vrochidou

Department of Electrical and Computer Engineering, Democritus University of Thrace, GR-67100 Xanthi, Greece, Tel.: +30 6947 181 886

#### evrochid@ee.duth.gr

Eleni Vrochidou received the Diploma, MSc, and PhD degrees from Democritus University of Thrace (DUTH), Xanthi, Greece, in 2004, 2007, and 2016, respectively. She is currently with the Laboratory of Electronics, Department of Electrical and Computer Engineering, DUTH. Her research interests are in signal processing, pattern recognition, and intelligent systems.

#### **Petros-Fotios Alvanitopoulos**

Department of Electrical and Computer Engineering, Democritus University of Thrace, GR-67100 Xanthi, Greece

Petros-Fotios Alvanitopoulos received the Diploma and PhD degrees from Democritus University of Thrace (DUTH), Xanthi, Greece, in 2005 and 2011, respectively. He is currently with the Laboratory of Electronics, Department of Electrical and Computer Engineering, DUTH. His research interests are mainly in signal processing, pattern recognition, and intelligent systems. Dr. Alvanitopoulos is a member of the Technical Chamber of Greece.

#### Ioannis Andreadis

Department of Electrical and Computer Engineering, Democritus University of Thrace, GR-67100 Xanthi, Greece

Ioannis Andreadis received the Diploma degree from the Department of Electrical and Computer Engineering, Democritus University of Thrace (DUTH), Xanthi, Greece, in 1983 (1978-1983 IKY Scholarship), and the MSc and PhD degrees from the University of Manchester, Manchester, UK, in 1985 and 1989, respectively. He joined the Department of Electrical and Computer Engineering, DUTH, in 1993. He supervised 9 PhD theses, 15 M.Sc. theses, and 56 Diploma dissertations. He is the author of an Institute of Physics "Select Paper" in 2010. He has published 200 referred publications in book chapters, international journals, and conferences. His research interests are mainly in electronic systems design, intelligent systems, and machine vision. Prof. is a Fellow of the Institution of Engineering and Technology (IET), London, UK. He has been an Associate Editor of the Pattern Recognition Journal since 1996 and a member of the Technical Chamber of Greece since 1983. He was a member of the Board of Governors of the European Commission Joint Research Center from 2008 to 2010. He has served as a Reviewer for leading scientific journals in his areas of interest and a member of Program Technical Committees of premier conferences such as ICIP and ICASSP. He was the recipient of the IET Image Processing Premium Award in 2009, the Best Paper Award (Computer Vision & Applications) in PSIVT 2007, and the Best Paper Award in EUREKA 2009.

#### Anaxagoras Elenas

Department of Civil Engineering, Democritus University of Thrace, GR-67100 Xanthi, Greece

Anaxagoras Elenas received the Diploma from the University of Stuttgart, Stuttgart, Germany, in 1984 and the Dr-Ing degree from Ruhr University, Bochum, Germany, in 1990. Since 1992, he has been a Faculty Member with the Department of Civil Engineering, Democritus University of Thrace, Xanthi, Greece, where he is currently an Associate Professor with the Institute of Structural Mechanics and Earthquake Engineering. His research interests are mainly in earthquake engineering and seismic signal processing. Dr. Elenas is a member of the Technical Chamber of Greece.